Localized orbital scaling correction for periodic systems

Aaron Mahler, Jacob Williams, Neil Qiang Su, and Weitao Yang

Localized orbital scaling correction for periodic systems

Aaron Mahler
Duke University, Department of Physics, Durham, NC 27708

Jacob Williams
Duke University, Department of Chemistry, Durham, NC 27708

Neil Qiang Su
Department of Chemistry, Key Laboratory of Advanced Energy Materials Chemistry (Ministry of Education) and
Renewable Energy Conversion and Storage Center (RECAST), Nankai University, Tianjin 300071, China and
Duke University, Department of Chemistry, Durham, NC 27708

Weitao Yang*
Duke University, Department of Chemistry, Durham, NC 27708 and
Duke University, Department of Physics, Durham, NC 27708
(Dated: June 13, 2022)

Density functional theory offers accurate structure prediction at acceptable computational cost, but commonly used approximations suffer from delocalization error; this results in inaccurate predictions of quantities such as energy band gaps of finite and bulk systems, energy level alignments, and electron distributions at interfaces. The localized orbital scaling correction (LOSC) was developed to correct delocalization error by using orbitals localized in space and energy. These localized orbitals span both the occupied and unoccupied spaces and can have fractional occupations in order to correct both the total energy and the one-electron energy eigenvalues. We extend the LOSC method to periodic systems, in which the localized orbitals employed are dually localized Wannier functions. In light of the effect of the bulk environment on the electrostatic interaction between localized orbitals, we modify the LOSC energy correction to include a screened Coulomb kernel. For a test set of semiconductors and large-gap insulators, we show that the screened LOSC (sLOSC) method consistently improves the band gap compared to the parent density functional approximation.

I. INTRODUCTION

The cost of solving the electronic Schrödinger equation scales exponentially with the size of the system, exceeding the computational resources available on the planet for any system larger than a few tens of electrons. [1] Density functional theory (DFT) sidesteps this exponential cost by treating the electron density as the fundamental variable instead of computing the wavefunction directly and by constructing an auxiliary noninteracting reference system sharing the density of the physical system. [2, 3] Due to the accuracy attainable at a cost only cubic in the number of electrons N, DFT has become a mainstay of computational chemistry and materials science. [4–7] While DFT is exact in theory, the form of the universal exchange-correlation functional is unknown, and density functional approximations (DFAs) must be used in practice. Commonly used DFAs suffer from systematic delocalization and static correlation errors. [8, 9] The delocalization error underlies the failure of DFAs to describe energy band gaps of finite and bulk systems, energy level alignments, and electron distributions at interfaces. [10] Overcoming delocalization error remains an active and challenging research effort.

Connecting single-particle orbital energies ϵ to observable quantities was another longstanding question in Kohn–Sham DFT. As a contrast, Koopmans [11] showed in 1934 that the Hartree–Fock ionization potential (IP) and electron affinity (EA) are given under the frozen orbital aproximation by the negative of the highest occupied and lowest unoccupied molecular orbital eigenvalues respectively. A series of three results established a rigorous connection for DFT.

First, Janak [12] derived a link between the Kohn–Sham orbital energies ϵ_m and the total energy E, viewed as a function of the orbital occupation numbers n_m:

$$\epsilon_m = \frac{\partial E}{\partial n_m}. \tag{1}$$

However, $\partial E/\partial n_m$ was not yet linked to a physical observable.

A few years later, Perdew, Parr, Levy, and Balduz [13] showed that E is piecewise linear in the number of electrons N when computed with the exact functional; that is, for all $|\delta| \leq 1$, we have

$$E(N + \delta) = \begin{cases} (1+\delta)E(N) - \delta E(N-1) & \delta < 0, \\ (1-\delta)E(N) + \delta E(N+1) & \delta \geq 0. \end{cases} \tag{2}$$

This relationship, called the PPLB condition, connects the chemical potential $\mu(N) = \partial E/\partial N$ to the IP and EA; observe that

$$\mu(N) = \begin{cases} -I(N) = E(N) - E(N-1) & \partial N < 0, \\ -A(N) = E(N+1) - E(N) & \partial N > 0. \end{cases} \tag{3}$$

* weitao.yang@duke.edu

Finally, Cohen *et al.* [14] proved that the chemical potential is given by the partial derivative of E with respect to the frontier orbital eigenvalues,

$$\mu(N) = \frac{\partial E}{\partial n_f}. \quad (4)$$

Crucially, f labels not only the highest unoccupied molecular orbital (HOMO) if $\partial N < 0$, but also the lowest unoccupied molecular orbital (LUMO) if $\partial N > 0$; this was the first time a physical meaning for the energy of the Kohn–Sham LUMO was established. This result holds for any local functional continuous in the electron density, as well as any nonlocal functional continuous in the Kohn–Sham density matrix; in the latter case, the work also extends Janak's theorem to the eigenvalues from the generalized Kohn–Sham equations.

Combining these three results, we see that

$$\mu(N) = \begin{cases} -I(N) = \epsilon_{\text{HOMO}} & \partial N < 0, \\ -A(N) = \epsilon_{\text{LUMO}} & \partial N \geq 0. \end{cases} \quad (5)$$

Thus, the frontier eigenvalues obtained from an N-electron DFT calculation correspond rigorously to physically relevant quantities;[14] if the PPLB condition is obeyed and the functional predicts the exact energies for $N-1$, N, and $N+1$ electrons, the correspondence is exact.

A feature derivable from these quantities is the fundamental or integer gap, defined as the difference between the IP and the EA:

$$\begin{aligned} E_{\text{gap}}^{\text{integer}} &= I - A \\ &= E(N-1) - 2E(N) + E(N+1). \end{aligned} \quad (6)$$

$E_{\text{gap}}^{\text{integer}}$ quantifies the difference between positively and negatively ionizing the system and is a crucial part of the accurate modeling of semiconductor electronic structure. If the PPLB condition is obeyed, Eqs. (3) and (5) also allow the gap to be computed from a single N-electron calculation as the discontinuity in the chemical potential; in this form, it is called the derivative gap, defined as

$$\begin{aligned} E_{\text{gap}}^{\text{deriv}} &= \left.\frac{\partial E}{\partial N}\right|_+ - \left.\frac{\partial E}{\partial N}\right|_- \\ &= \epsilon_{\text{LUMO}} - \epsilon_{\text{HOMO}}. \end{aligned} \quad (7)$$

If the PPLB condition is obeyed, the derivative gap and the integer gap are equal.[14] In bulk systems with periodic boundary conditions, the PPLB condition is satisfied by any DFA continuous in the Kohn–Sham density or density matrix, regardless of systematic errors in its definition; [10] thus, the fundamental gap of bulk systems can be predicted by the (generalized) Kohn–Sham orbital gap, for functionals continuous in the density (density matrix), as in Eq. (7). In finite systems, however, the PPLB condition is not in general obeyed, and the gap computed from Eq. (7) may differ from that computed by calculating the $(N\pm1)$-electron energies to obtain the integer gap as in Eq. (6), the ΔSCF method.

A. Delocalization error

The delocalization error has a dramatic size-dependent manifestation. In finite systems, standard DFAs fail to obey the PPLB linearity condition, so the derivative gap is not equal to the integer gap. This is due to the error in the approximate exchange-correlation functional, which nearly always yields E convex in N, underestimating the piecewise linearity prescribed by the PPLB condition. This convex deviation has been identified as the cause for an unphysical smearing of the electron density in space, as well as underestimation of the total energy in a delocalized electron density; thus, we may identify it with delocalization error, as exhibited in small systems. In bulk systems, the delocalized nature of the orbitals produces a total energy linear with respect to fractional charge, yielding no deviation from the PPLB condition; however, delocalization error manifests as an incorrect slope of the $E(N)$ line at integer N. [10]

The effects of delocalization error include the underestimation of band gaps and reaction barriers, [15] undervaluation of dissociation curves, [16–18] overestimation of conductance and polarizability, [19] and incorrect energy level alignment and charge transfer across interfaces. [20, 21] To capture the full derivative discontinuity and hence the band gap, it has been shown that the exact functional, whether local or nonlocal, cannot be a differentiable functional of the electron density or of the Kohn-Sham density matrix. [22, 23] To reduce the systematic delocalization error, many approaches have been developed, including range-separated functionals, [24–30] the screened range-separated hybrid functional, [31] self-interaction error corrected functionals, [17, 32–38] Koopmans-compliant functionals, [39, 40] and generalized transition state methods, [41] along with related developments using localized Wannier functions. [42]

The localized orbital scaling correction (LOSC) method was developed to eliminate delocalization error systematically. [43, 44] Previous incarnations of LOSC were implemented for molecular systems with real orbitals and the boundary condition $\lim_{|\mathbf{r}|\to\infty} \rho(\mathbf{r}) = 0$. They accurately model IP, EA, photoemission spectra, dissociation curves, and polarizabilities, as well as restore size-consistency. [43–46] In this work, we extend LOSC to periodic boundary conditions (PBCs) and complex orbitals. Additionally, we introduce a screened Coulomb interaction to the LOSC energy correction to enable the accurate computation of bulk system band structures.

B. Periodic boundary conditions

In PBCs, the eigenfunctions of the single-particle Hamiltonian are known as Bloch orbitals; they satisfy $h_s|\psi_n^{\mathbf{k}}\rangle = \epsilon_n^{\mathbf{k}}|\psi_n^{\mathbf{k}}\rangle$. The Bloch orbitals are also eigenfunctions of the unit cell translation operator, so they take the form $|\psi_n^{\mathbf{k}}\rangle = e^{i\mathbf{k}\cdot\mathbf{r}}|u_n^{\mathbf{k}}\rangle$, where $|u_n^{\mathbf{k}}\rangle$ has the periodicity of the unit cell and $\mathbf{k}$ is a point in the Brillouin zone (the reciprocal-space unit cell). [47, 48] The Bloch

orbitals obey the normalization convention $\langle\psi_m^{\mathbf{q}}|\psi_n^{\mathbf{k}}\rangle = \delta(\mathbf{k}-\mathbf{q})\delta_{mn}$, where $\langle f|g\rangle = \int_{\mathcal{D}} d\mathbf{r}\,\overline{f}(\mathbf{r})g(\mathbf{r})$. Here, $\delta(\mathbf{k})$ is the Dirac delta distribution, δ_{mn} is the Kronecker delta, and $\overline{f}$ is the complex conjugate of f. The domain of integration $\mathcal{D}$ is the periodic unit for the functions being integrated; for Bloch orbitals, $\mathcal{D} = \mathbb{R}^3$. The $|u_n^{\mathbf{k}}\rangle$ are orthonormal in the band index n at a fixed $\mathbf{k}$-point in reciprocal space: that is, $\langle u_m^{\mathbf{k}}|u_n^{\mathbf{k}}\rangle = \delta_{mn}$, where the inner product integrates over one unit cell. Note that we assume closed-shell systems in this work.

The single-particle density can be represented in real space by the occupied Bloch orbitals as

$$\rho_s(\mathbf{r}) = \sum_n^{\text{occ}} \frac{V}{(2\pi^3)} \int_{\text{BZ}} d\mathbf{k}\,|\psi_n^{\mathbf{k}}(\mathbf{r})|^2, \qquad (8)$$

where V is the volume of the unit cell and the integral is over the first Brillouin zone. Since the Hamiltonian is diagonal in $\mathbf{k}$, we can solve for the Bloch orbitals in reciprocal space, requiring diagonalization only in one unit cell. In practice, the Brillouin zone is sampled with a finite number of points; in this work we use a Monkhorst–Pack mesh centered at the origin Γ of the Brillouin zone. [49] Thus, integrals over the Brillouin zone become equally weighted sums over the $\mathbf{k}$-mesh

$$\frac{V}{(2\pi)^3} \int d\mathbf{k}\,f(\mathbf{k}) \mapsto \frac{1}{N_k} \sum_{\mathbf{k}} f(\mathbf{k}), \qquad (9)$$

where N_k is the number of $\mathbf{k}$-points in the mesh. Using a Monkhorst–Pack mesh centered at Γ yields Bloch orbitals having the periodicity of an unfolded supercell comprised of N_k primitive unit cells; this supercell is referred to as the Born–von Karman cell. [48] The Bloch orbitals then obey the normalization convention $\langle\psi_m^{\mathbf{q}}|\psi_n^{\mathbf{k}}\rangle = N_k\delta_{\mathbf{k}\mathbf{q}}\delta_{mn}$, where the integral is over the Born–von Karman cell.

II. METHODS

The LOSC method consists of two steps. First, we find orbitals that are spatially localized while remaining associated with specific energy ranges. Next, we compute a curvature matrix modeling the magnitude of the deviation from linearity. This is combined with the fractionally occupied localized orbitals to correct the convex deviation of $E(N)$ from linearity at non-integer N, as well as incorrect total energies at integer N. Both steps are implemented as post-processing after a converged self-consistent field calculation.

A. Localization

The wave-like nature of the Bloch orbitals prohibits them from being spatially localized. In order to obtain a state that is localized in space, the discrete Fourier transform of the Bloch orbitals is used to produce Wannier functions [50]

$$|w_n^{\mathbf{R}}\rangle = \frac{1}{N_k} \sum_{\mathbf{k}} e^{-i\mathbf{k}\cdot\mathbf{R}}|\psi_n^{\mathbf{k}}\rangle. \qquad (10)$$

Wannier functions inherit the periodicity of the Born–von Karman cell, and are indexed by electron bands n and unit cells $\mathbf{R}$ in the supercell. They are symmetric under translation by unit cell vectors, so that $w_n^{\mathbf{R}}(\mathbf{r}) = w_n^{\mathbf{0}}(\mathbf{r}-\mathbf{R})$; $\mathbf{R} = \mathbf{0}$ is referred to as the home unit cell. There is a unitary, or gauge, freedom at each $\mathbf{k}$-point in the choice of Bloch orbitals that comprise a Wannier function, so we can define *generalized* Wannier functions [51]

$$\begin{aligned} |w_i^{\mathbf{R}}\rangle &= \frac{1}{N_k} \sum_{\mathbf{k}} e^{-i\mathbf{k}\cdot\mathbf{R}} \sum_n U_{ni}^{\mathbf{k}}|\psi_n^{\mathbf{k}}\rangle \\ &= \frac{1}{N_k} \sum_{\mathbf{k}} e^{-i\mathbf{k}\cdot\mathbf{R}}|\phi_i^{\mathbf{k}}\rangle, \end{aligned} \qquad (11)$$

where we refer to $|\phi_i^{\mathbf{k}}\rangle$ as a transformed Bloch orbital (TBO). From now on, we will refer to generalized Wannier functions as Wannier functions.

The gauge freedom $U^{\mathbf{k}}$ in the TBOs can be chosen such that the resulting set of Wannier functions have advantageous properties. In order to obtain localization in space, Marzari and Vanderbilt suggested choosing $U^{\mathbf{k}}$ that minimize the Wannier functions' spatial variance $\langle\Delta r^2\rangle_i = \langle r^2\rangle_i - \langle\mathbf{r}\rangle_i^2$, where $\langle x\rangle_i = \langle w_i^{\mathbf{0}}|x|w_i^{\mathbf{0}}\rangle$; the resulting orbitals are called maximally localized Wannier functions. [52] In molecules, the scheme of minimizing spatial variance is referred to as Foster–Boys localization. [53] However, constructing maximally localized Wannier functions from both valence and conduction bands is physically ill-motivated. Because bands far apart in energy can mix freely and the Bloch bands form a complete basis, adding more virtual bands will result in increasing spatial localization of the maximally localized Wannier functions, with a corresponding loss of information about the energy dispersion of the bands.

In order to preserve locality in energy while maintaining spatial localization, enabling simultaneous treatment of the occupied and unoccupied spaces, we choose the Wannier gauge that minimizes a cost function considering both energy and spatial variance:

$$F = (1-\gamma)\sum_i \langle\Delta r^2\rangle_i + \gamma C \sum_i \langle\Delta h_s^2\rangle_i, \qquad (12)$$

where $0 \le \gamma \le 1$ and in the units used here $C = 1\,\text{a}_0^2/\text{eV}^2$, where a_0 is the Bohr radius. This cost function was first proposed by Gygi *et al.* [54] for computations sampling the Brillouin zone only at Γ and implemented for such systems by Giustino and Pasquarello [55]. It was used for LOSC in molecules [44] to treat system symmetries and degeneracies more robustly than the original localization, which used soft energy windows; [43] in molecular LOSC, the localized orbitals are called *orbitalets*. We recently extended F to systems with $N_k \ge 1$; [56] we refer to

such orbitals as dually localized Wannier functions (DL-WFs). These formulations show how the combination of occupied and unoccupied spaces can be localized simultaneously to produce Wannier functions that are localized in both space and energy. This construction is critical for addressing delocalization error in finite systems because it allows for dynamic localization in the resulting orbitals; the orbitals can qualitatively and quantitatively differ depending on the geometry of the system. [43, 44] In keeping with the principle of universality in functional development, we use the same mixing parameter in Eq. (12), setting $\gamma = 0.47714$. The value of γ has important implications for the LOSC method; see Section VI of the Supplementary Information of Su *et al.* [44]. Setting $\gamma = 0$, for instance, yields maximally localized Wannier functions, [52] while $\gamma = 1$ yields DLWFs that are pure Fourier transforms (up to $\mathbf{k}$-dependent phases) of the Kohn–Sham bands.

Note that we have not proven that a unique global minimum of F exists; in practice, F has a fairly rugged landscape of solutions, and we have observed multiple local minima. We choose the DLWFs yielding the smallest total cost. Different DLWFs can produce somewhat different sLOSC corrections, with eigenvalues varying by up to a few tenths of an eV. The problem of multiple minima of F has also been observed in molecular LOSC, [57] but was not found to be the dominant source of error. An additional question worth exploring is the effect of symmetry breaking, such as that due to perturbations of the crystal lattice, on the localization procedure.

The compromise between spatial and energy localization and the inclusion of unoccupied orbitals are key to producing localized orbitals that can address delocalization error while retaining size-consistency. For example, the DFA HOMO and LUMO of H_2^+ at (or near) the dissociation limit are delocalized over the whole molecule; since they are (nearly) degenerate, there exists a unitary freedom in the subspace spanned by both. Due to the symmetry of the system, we expect to obtain two separate $H^{0.5+}$ fragments; the (small or) vanishing gap means that any choice of $\gamma < 1$ in Eq. (12) will result in half-occupied orbitals localized on each H atom. This is the physical motivation for a localization scheme that minimizes the spatial variance of occupied and unoccupied orbitals while allowing only orbitals that are close in energy to mix. [43]

B. Energy corrections

The deviation from energy linearity with respect to fractional charges is characteristically quadratic in most exchange-correlation functionals. [43, 58, 59] To restore compliance with the PPLB condition for small finite systems, the global scaling correction (GSC) was developed. GSC corrects the total energy by an amount quadratic in the occupation numbers of the canonical molecular orbitals. [58, 60] This method is effective at correcting the systematic deviation from the PPLB condition

for systems with fractional charges and leads to accurate prediction of quasiparticle energies as the eigenvalues from the resulting one-electron Hamiltonian. However, GSC is applicable only for systems of small and moderate size; the convex deviation of conventional DFAs from the piecewise linearity prescribed by the PPLB condition decreases with increasing system size, and the delocalization error manifests instead as underestimated ground-state energies for integer systems and incorrect linear $E_{gs}(N)$ curves with wrong slopes at the bulk limit. [10] The localized orbital scaling correction (LOSC) applies its energy correction adaptively by the construction of localized orbitals, allowing systematic and size-consistent correction of delocalization error. [43, 44] In this section, we discuss the extension of LOSC to periodic systems.

A basic quantity in LOSC is the density matrix in the basis of DLWFs; its elements are occupations

$$\lambda_{ij}^{\mathbf{TR}} = \langle w_i^{\mathbf{T}} | \rho_s | w_j^{\mathbf{R}} \rangle. \quad (13)$$

The occupations between all pairs of DLWFs are used to remove quadratic deviations, while the diagonal terms are used to restore linearity. The energy correction defined by LOSC for each unit cell is given by

$$\Delta E^{\text{LOSC}} = \frac{1}{2N_k} \sum_{\mathbf{TR}} \sum_{ij} \widetilde{\kappa}_{ij}^{\mathbf{TR}} \lambda_{ij}^{\mathbf{TR}} (\delta_{ij}^{\mathbf{TR}} - \overline{\lambda}_{ij}^{\mathbf{TR}}), \quad (14)$$

where $\delta_{ij}^{\mathbf{0R}} = \delta_{ij}\delta_{\mathbf{0R}}$; $\widetilde{\kappa}$ models the curvature of the deviation from linearity.

The diagonal terms in the energy correction are proportional to $\lambda_{ii}^{\mathbf{TR}} - |\lambda_{ii}^{\mathbf{TR}}|^2$; thus, if a DLWF has integer occupancy (implying $\lambda_{ij}^{\mathbf{TR}} = 0$ whenever $i \neq j$ or $\mathbf{T} \neq \mathbf{R}$), then the energy correction due to that DLWF will also be zero.

The matrix $[\lambda_{ij}^{\mathbf{TR}}]$ of occupations between the DLWFs is the discrete Fourier transform of the occupation matrix between the TBOs. As such, it is positive semidefinite and Hermitian, and

$$\text{tr}_c[\lambda_{ij}^{\mathbf{TR}}] = \frac{1}{N_k} \sum_{\mathbf{k}} N_f^{\mathbf{k}}, \quad (15)$$

where tr_c denotes the trace per unit cell and $N_f^{\mathbf{k}}$ is the number of electrons below the Fermi energy at $\mathbf{k}$.

Following Su *et al.* [44], the elements of the curvature matrix are given by

$$\begin{aligned} \widetilde{\kappa}_{ij}^{\mathbf{TR}} = {}& \text{erf}(8S_{ij}^{\mathbf{TR}})\sqrt{\kappa_{ii}^{\mathbf{TT}}\kappa_{jj}^{\mathbf{RR}}} \\ & + \text{erfc}(8S_{ij}^{\mathbf{TR}})\kappa_{ij}^{\mathbf{TR}}. \end{aligned} \quad (16)$$

Here, $\text{erfc}(r) = 1 - \text{erf}(r)$ is the complementary error function. $S_{ij}^{\mathbf{TR}}$ is the absolute overlap between DLWFs,

$$S_{ij}^{\mathbf{TR}} = \int d\mathbf{r} \sqrt{\rho_i^{\mathbf{T}}(\mathbf{r})\rho_j^{\mathbf{R}}(\mathbf{r})}, \quad (17)$$

where $\rho_i^{\mathbf{T}}(\mathbf{r}) = |w_i^{\mathbf{T}}(\mathbf{r})|^2$ is a DLWF's charge density. The matrix elements $\kappa_{ij}^{\mathbf{TR}}$ in Eq. (16) are given by

$$\kappa_{ij}^{\mathbf{TR}} = J[\rho_i^{\mathbf{T}}, \rho_j^{\mathbf{R}}] - X[\rho_i^{\mathbf{T}}, \rho_j^{\mathbf{R}}], \quad (18)$$

with

$$J[\rho_i^{\mathbf{T}}, \rho_j^{\mathbf{R}}] = \iint d\mathbf{r}\, d\mathbf{r}'\, \rho_i^{\mathbf{T}}(\mathbf{r})\rho_j^{\mathbf{R}}(\mathbf{r}')K(|\mathbf{r}-\mathbf{r}'|), \quad (19a)$$

$$X[\rho_i^{\mathbf{T}}, \rho_j^{\mathbf{R}}] = \tau\frac{2C_{\mathrm{X}}}{3}\int d\mathbf{r}\left[\rho_i^{\mathbf{T}}(\mathbf{r})\rho_j^{\mathbf{R}}(\mathbf{r})\right]^{2/3}. \quad (19b)$$

In the above, $K(r) = 1/r$ is the Coulomb kernel, $C_X = \frac{3}{4}(\frac{6}{\pi})^{1/3}$ is the Dirac exchange constant, [61] and $\tau = 6(1-2^{-1/3}) \approx 1.2378$ is a nonempirical parameter.[43] The derivation of how this correction restores the PPLB condition can be found in the supplementary data of Li *et al.* [43]. The use of $\widetilde{\kappa}$ instead of κ was introduced because the cost function in Eq. (12) can induce discontinuous jumps between localization characters during molecular dissociation.[44] The diagonal elements of $\widetilde{\kappa}$ and κ are equal, so when $\lambda_{ii} \in \{0,1\}$ the corrections from $\widetilde{\kappa}$ and κ are the same. In practice, $X[\rho_i^{\mathbf{T}}, \rho_j^{\mathbf{R}}]$ term is evaluated using numerical integration on a grid of real-space points. The Coulomb term $J[\rho_i^{\mathbf{T}}, \rho_j^{\mathbf{R}}]$ is evaluated in a plane wave basis, detailed in Sec. II C.

Applying the extension of Janak's theorem[12] to the generalized Kohn-Sham theory, [14] the LOSC energy correction of Eq. (14) yields corrections to the Bloch orbital energy eigenvalues $\epsilon_n^{\mathbf{k}}$ given by

$$\Delta\epsilon_n^{\mathbf{k}} = \sum_i \widetilde{\kappa}_{ii}^{\mathbf{00}}\left(\frac{1}{2} - \lambda_{ii}^{\mathbf{00}}\right)|U_{ni}^{\mathbf{k}}|^2$$
$$- \sum_{\mathbf{R}i\neq\mathbf{0}j} \widetilde{\kappa}_{ij}^{\mathbf{0R}}\mathrm{Re}\left\{\lambda_{ij}^{\mathbf{0R}}e^{i\mathbf{k}\cdot\mathbf{R}}\overline{U}_{ni}^{\mathbf{k}}U_{nj}^{\mathbf{k}}\right\}. \quad (20)$$

Consider the diagonal corrections given by the first summand in Eq. (20). There is no correction to the eigenvalue when a DLWF is half-occupied ($\lambda_{ii} = \frac{1}{2}$); on the other hand, the correction is maximal when it is completely occupied or unoccupied. Li *et al.* [43] observed that the slopes of the quadratic DFA and the correct linear $E(N)$ curves agree at half-integer N. Since the frontier orbital energy corresponds to this slope, we see that accurate frontier orbital energies are given by half-occupied frontier orbitals. The LOSC correction to the orbital energies arrives naturally at this conclusion, additionally agreeing with Slater transition state theory. [62, 63]

We may also view LOSC as a correction to the Kohn–Sham Hamiltonian. It is given by the functional derivative of the energy correction with respect to the density operator under the frozen orbital approximation,

$$\Delta v = \left.\frac{\delta\Delta E^{\mathrm{LOSC}}}{\delta\rho_s}\right|_{\{w_i^{\mathbf{R}}\}}, \quad (21)$$

and can be written in operator form as

$$\Delta v = \sum_{ij,\mathbf{TR}} \widetilde{\kappa}_{ij}^{\mathbf{TR}}\left(\frac{\delta_{ij}^{\mathbf{TR}}}{2} - \lambda_{ij}^{\mathbf{TR}}\right)|w_i^{\mathbf{T}}\rangle\langle w_j^{\mathbf{R}}|. \quad (22)$$

(See the Supplemental Material [64] for details on this derivation.) The correction to the nth Bloch orbital eigenvalue is then given by $\Delta\epsilon_n^{\mathbf{k}} = \langle\psi_n^{\mathbf{k}}|\Delta v|\psi_n^{\mathbf{k}}\rangle$.

In practice, the energy corrections are applied to disentangled Bloch orbitals. The conduction bands of most systems cannot be formed into sets of bands that do not cross anywhere in the Brillouin zone, a condition referred to as band entanglement. In order to obtain a finite set of bands for localization and energy correction, we use the disentanglement procedure outlined by Souza *et al.* [65] This procedure obtains N_w bands from a set of $N_b \geq N_w$ Bloch orbitals at each $\mathbf{k}$-point, chosen such that the subspace spanned by the disentangled bands is as smooth as possible in $\mathbf{k}$. To correct the band gap of semiconductors and insulators, we include sufficiently many virtual bands in the construction of the Wannier functions to converge the localization of the frontier bands (that is, the valence band maximum and conduction band minimum). [56] We find that $N_b = N_{\mathrm{occ}} + 3N_{\mathrm{coord}}$ and $N_w = N_{\mathrm{occ}} + 2N_{\mathrm{coord}}$, where N_{occ} is the number of occupied bands per unit cell and N_{coord} is the coordination number of the lattice, are sufficient; see the Supplemental Material for details. The N_w disentangled Bloch bands yield N_w DLWFs per unit cell, so there are $N_w N_k$ DLWFs in the Born–von Karman supercell on which they are periodic. The energy corrections for the N_w disentangled Bloch rbitals at each $\mathbf{k}$-point are implemented using Eq. (20).

In this work, we restrict our attentions to closed-shell systems. Extending the LOSC method to spin-polarized materials is accomplished by finding the corrections from the spin-up and spin-down DLWFs independently and summing them to obtain ΔE^{LOSC}; this functionality is planned for the next version of LOSC. However, treating the strong correlation common to open-shell materials brings its own set of challenges beyond the scope of this work. We discuss them briefly in Sec. IV below.

C. Coulomb integrals

Accurate calculation of the Coulomb interaction $J[\rho_i^{\mathbf{T}}, \rho_j^{\mathbf{R}}]$ is needed for LOSC to restore the PPLB condition. In PBCs, a plane-wave basis is typically employed. The Coulomb energy is diagonal in this basis, and the double integral required in real space collapses to a single sum over basis vectors $\mathbf{G}$:

$$J[\rho_i^{\mathbf{T}}, \rho_j^{\mathbf{R}}] = \sum_{\mathbf{G}} \frac{4\pi}{G^2}\bar{\rho}_i^{\mathbf{T}}(\mathbf{G})\rho_j^{\mathbf{R}}(\mathbf{G}), \quad (23)$$

where $G = |\mathbf{G}|$. However, this sum converges only for neutral charge distributions, for which the $\mathbf{G} = \mathbf{0}$ term vanishes. The DLWF densities are individually charged, so ignoring the divergent term coming from the net charge will significantly underestimate the Coulomb energy. There are many methods to evaluate the Coulomb energy for charged densities in the plane-wave basis accurately, including those of Makov and Payne [66], Kantorovich [67], Dabo *et al.* [68], and Li and Dabo [69]. We choose the spherical cutoff method, [70–72] truncating the Coulomb kernel in Eq. (19a) at a cutoff radius R_c; this is taken to be half the length of the shortest Born–von Karman supercell lattice vector, ensuring that the

Coulomb interactions between the a DLWF density and its images in neighboring supercells are zero. Thus, the spherical cutoff Coulomb kernel is

$$K_c(r; R_c) = \begin{cases} 1/r & r < R_c \\ 0 & r \geq R_c, \end{cases} \quad (24)$$

which has Fourier coefficients

$$K_c(G; R_c) = \begin{cases} \dfrac{4\pi}{G^2}[1 - \cos(GR_c)] & G \neq 0 \\ 2\pi R_c^2 & G = 0. \end{cases} \quad (25)$$

Observe that $K_c(G; R_c)$ does not diverge for any $\mathbf{G}$. As long as the pair of DLWF densities in Eq. (19a) lie in a sphere of radius R_c, the spherical cutoff method is also accurate in highly anisotropic unit cells, unlike schemes such as that of Makov and Payne. [67] We enforce this containment condition in practice by checking that each DLWF density is well contained in a volume spanned by half of each Born–von Karman supercell lattice vector, and only compute curvature elements between pairs of DLWF densities that have centers closer together than R_c. We evaluate the Coulomb integrals on the unfolded supercell in the plane-wave basis, which requires a fast Fourier transform (FFT) of the DLWF densities on the supercell.

D. Screening

Applying LOSC with a bare Coulomb interaction leads to severe overcorrection of semiconductors' band gaps in PBCs. However, this is not surprising; we anticipate an effect of the other electrons in the lattice on $J[\rho_i^{\mathbf{T}}, \rho_j^{\mathbf{R}}]$. As shown by highly accurate methods such as GW, a screened Coulomb interaction is required to model the interaction between electrons in a periodic system accurately. [73, 74] Recently, Mei and coworkers also found that the deviation from linearity of the total energy as a function of canonical orbital occupations is given to second order by a screened interaction. [60] We model the screening phenomenologically, attenuating the long-range $1/r$ behavior of the spherical cutoff Coulomb interaction by a complementary error function. This modifies the Coulomb kernel to read

$$K_s(r; R_c, \alpha) = \begin{cases} \operatorname{erfc}(\alpha r)/r & r < R_c \\ 0 & r \geq R_c, \end{cases} \quad (26)$$

where α is a screening parameter. We choose the α that best reproduces the experimental band gaps of a test set of semiconductors and insulators. For r larger than the screening radius α^{-1}, $K_s(r; R_c, \alpha)$ decays exponentially instead of as $1/r$. The Fourier coefficients of K_s are

$$K_s(G; R_c, \alpha) = \begin{cases} \dfrac{4\pi}{G^2}\left[1 - \cos(GR_c)\operatorname{erfc}(\alpha R_c) - e^{-(G/2\alpha)^2}\operatorname{Re}\left\{\operatorname{erf}\left(\alpha R_c + \dfrac{iG}{2\alpha}\right)\right\}\right] & G \neq 0 \\ 2\pi R_c^2 + \pi\operatorname{erf}(\alpha R_c)\left(\alpha^{-2} - 2R_c^2\right) - 2\sqrt{\pi}e^{-(\alpha R_c)^2}R_c/\alpha & G = 0. \end{cases} \quad (27)$$

The error function is unbounded for complex arguments, overflowing double-precision floating-point numbers even for relatively small G. Thus, we evaluate $K_s(G; R_c, \alpha)$ with a scaled form of erf z called the Faddeeva function, implemented in the numerically stable ACM Algorithm 916. [75, 76] For details, see the Supplemental Material.

In principle, the screening is system-dependent. Improved accuracy would be attainable by setting its value to best reproduce each material's band gap. However, the phenomenological screening model of sLOSC does not enable doing so while retaining predictive ability. This would require a rigorously screened Coulomb (or Hartree-exchange-correlation) interaction based on the linear response function $\chi(\mathbf{r}, \mathbf{r}') = \delta\rho_s(\mathbf{r})/\delta v(\mathbf{r}')$. *Ab initio* screening of this kind appears in the extensions of the GSC method to hybrid functionals [77] and in the following exploration of orbital relaxation on GSC, [78] the GSC2 method, [60] as well as in recent work on Koopmans-compliant functionals. [79–81] For small, finite systems, the delocalization error is quanti-

fied by $\partial^2 E/\partial n_i^2$, where n_i is the occupation number of the Kohn–Sham orbital $|\psi_i\rangle$; analytical expressions for $\partial^2 E/\partial n_i^2$ were derived in Yang *et al.* [82] In sLOSC, linear-response screening would very likely increase the accuracy, but at substantial computational cost to compute the nonlocal $\chi(\mathbf{r}, \mathbf{r}')$.

III. RESULTS

We use the PBE functional [6] for the parent DFA calculations, with optimized norm-conserving Vanderbilt pseudopotentials [83] generated by PseudoDojo. [84] Both self-consistent field (SCF) and non-SCF calculations are carried out in the `Quantum ESPRESSO` code suite. [85, 86]

The energy cutoff for the fast Fourier transform is set to 100 Ry for wavefunctions and 400 Ry for densities. The Brillouin zone is sampled with Monkhorst–Pack meshes centered at Γ, which is necessary for the Wannier func-

tions to be periodic on the Born–von Karman supercell. For SCF calculations, we use a $16\times16\times16$ **k**-mesh, while the other calculations are performed on $6\times6\times6$ grids. The localization step of LOSC is implemented in a modified fork of the `wannier90` code, [87–89] and the energy correction as module to a fork of `Quantum ESPRESSO`.

To determine an optimal screening parameter α, we minimize the mean absolute percent error (MAPE) on the SC/40 set of semiconductors with experimentally available band gaps [90] together with six additional large-gap insulators. The experimental band gaps studied range from $0.23\,\text{eV}$ to $21.7\,\text{eV}$. We find that $\alpha = 0.15\,\text{a}_0^{-1}$ achieves the lowest MAPE; coincidentally, this value is numerically equal to the screening parameter used in the HSE density functional. [90] As shown in Fig. 1, LOSC with Coulomb screening (sLOSC) yields marked improvement of the band gap for the test set in comparison with the parent functional. It is also apparent that unscreened LOSC overcorrects the band gaps; indeed, it is less accurate than the parent functional. The performance of sLOSC in molecules is better than the parent functional, but unscreened LOSC achieves the best performance in molecular systems (see Table I). The Supplemental Material details the variation in performance of screened LOSC for both bulk systems and molecules with the screening parameter α.
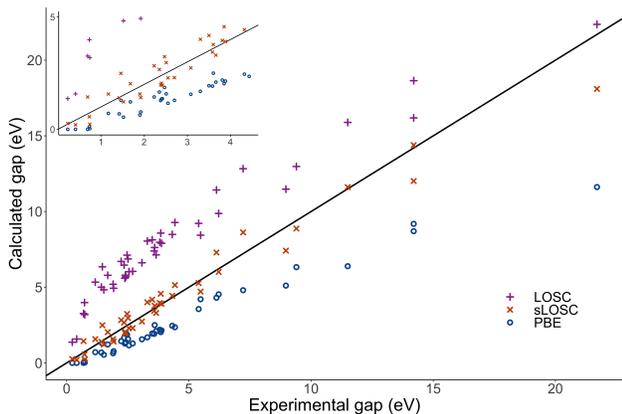
Figure 1. Comparison of experimental band gaps with those calculated by PBE (o), sLOSC ($\times$), and unscreened LOSC (+). The inset shows systems with an experimental band gap less than $5\,\text{eV}$.

Table I. Mean absolute percent error of the band gap for PBC and molecular test sets. For details on the systems tested, see the Supplemental Material.

Method	PBE	LOSC	sLOSC
PBC	47.5%	158.6%	19.7%
Molecule	79.8%	10.1%	43.6%

The band structures of sLOSC and of the parent functional are shown for the small-gapped semiconductor silicon in Fig. 2 and the larger-gapped insulator lithium

fluoride in Fig. 3. They use the disentangled band structures, which are numerically indistinguishable from the true band structure at and below the conduction band minimum for the parent functional. Wannier interpolation in the same DLWF basis as that used in sLOSC is used to find the energy at the points in the Brillouin zone not explicitly treated by the localization and energy correction. The sLOSC correction to the band structure comes largely from the more localized DLWFs, for which there is a larger Coulomb self-energy $J[\rho_i^{\mathbf{R}}, \rho_i^{\mathbf{R}}]$. Because of this, sLOSC mostly corrects the energy of the occupied bands (which we observe to correspond closely to the occupied DLWFs in semiconductors); it affects the virtual bands much less. More work on molecule-surface and surface-surface interactions is required to determine whether LOSC yields correct energy level alignment and whether the larger correction to the valence bands is physically meaningful.
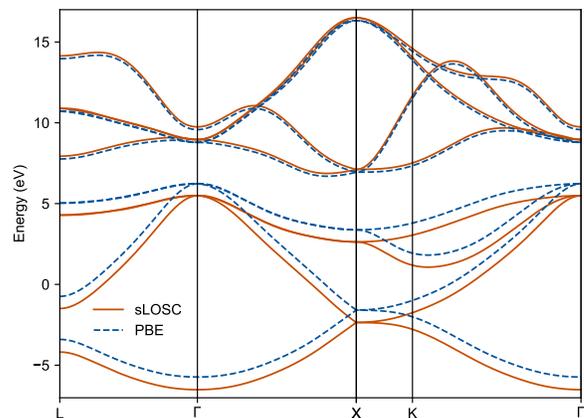
Figure 2. Band structure of silicon under the PBE functional (dashes) and sLOSC (solid). The Fermi energy of the PBE calculation was $6.23\,\text{eV}$, while the PBE with LOSC Fermi energy was $5.49\,\text{eV}$.

IV. DISCUSSION

We have shown that despite the simple form of its phenomenological Coulomb screening, sLOSC systematically corrects the band gap error associated with the parent functional for materials spanning a large range of band gaps. Screening improves the correction of delocalization error in bulk systems, but degrades the accuracy of molecular systems' band gaps relative to unscreened LOSC; however, sLOSC still offers better band gaps than those computed by the parent functional. One key remaining challenge is to model the curvature more accurately for all systems; we expect that linear response of the electron density, used by Mei *et al.* [60] for accurate screening of the Kohn–Sham orbitals, could be used to find the exact expression for $\partial^2 E/\partial\lambda_{ij}$. This would alleviate the error imposed by modeling κ as a difference between Coulomb repulsion and Dirac exchange.
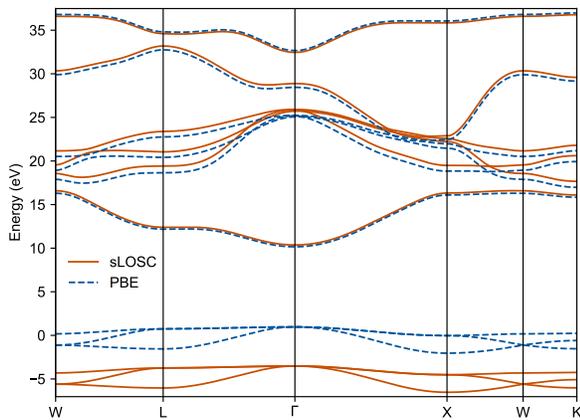
Figure 3. Band structure of lithium fluoride under the PBE functional (dashes) and sLOSC (solid). The Fermi energy of the PBE calculation was 0.97 eV, while the PBE with LOSC Fermi energy was -3.52 eV. The core states are not included in the figure.

We implement the energy correction as a post-processing step to a self-consistent calculation; such corrections are accurate when the change in electron density is small and hence the total energy correction is small. For every system considered in this work, ΔE^{LOSC} does not exceed three parts in 10^5. The corresponding change to the density for such systems is also expected to be minimal. LOSC can also be implemented self-consistently; [45] this can correct the delocalization error of the total density, improving the accuracy of LOSC for systems with large total energy corrections. A self-consistent implementation of sLOSC could be necessary for the accurate computation of heterogeneous and interfacial systems. Since delocalization error leads to incorrect charge distributions, the sLOSC energy correction is likely to be larger, and self-consistently correcting the delocalized density is expected to yield better orbital energies.

Work is ongoing to implement sLOSC for spin-polarized materials and to investigate its treatment of metals. The DLWFs of gapless systems constructed from Bloch bands near the Fermi energy are expected to have occupations λ_{ii} close to $\frac{1}{2}$, which means that the sLOSC correction to those eigenvalues will be small. While there may be changes to the overall band structure, it is likely that such systems will remain gapless.

This may not hold in semimetals, whose valence and conduction bands cross only in a small volume (or a single point) of the Brillouin zone. Metals, on the other hand, have one band that crosses the Fermi energy. sLOSC can open a gap in systems the DFA predicts to be semimetals; this occurs with the smallest-gapped system in our test set, InSb. Thus, it is not certain that true semimetals would remain so after the sLOSC correction. In addition, the treatment of strong correlation due to (near) degeneracy of spin states and the inclusion of topological or spin-orbit effects are beyond the scope of the current work. A modification of molecular LOSC to include fractional spins was developed in Su *et al.* [91]; it could

possibly be extended to bulk materials as well.

A. Comparison with other methods

1. DFT+U(+V)

(s)LOSC is related to the DFT+U [92, 93] method for correcting delocalization error. The kinship can be seen in the similarity of the sLOSC energy correction, Eq. (14), to the rotationally invariant DFT+U correction [94]

$$\Delta E_{\mathrm{DFT+U}} = \frac{1}{2} \sum_{\ell,\sigma} \mathrm{tr}\left[\boldsymbol{n}_{\ell\sigma}(1 - \boldsymbol{n}_{\ell\sigma}) \right] U_\ell, \qquad (28)$$

where U_ℓ is the effective Hubbard parameter for orthonormal local orbital (LO) ℓ, combining atom and orbital indices, and $\boldsymbol{n}_{\ell\sigma}$ is the LO occupation matrix. Both offer an adjustment to the total energy quadratic in the occupation of the LOs. The energy correction of DFT+U comes only from interactions between LOs on the same atom, although DFT+U+V [95] extends this to interactions between atoms, analogous to the off-diagonal curvature elements $\widetilde{\kappa}_{ij}$ of (s)LOSC. However, the LOs of DFT+U(+V) are static (usually being d and f orbitals on transition metal centers), while the DLWFs of sLOSC dynamically localize based on the gauge set by the cost function F. Thus, where DFT+U(+V) must recompute the effective Hubbard parameter for every perturbation of the crystal structure or molecular geometry, the size of the correction in (s)LOSC follows from the DLWFs.

It is worth noting that, while DFT+U(+V) does not explicitly include energy localization in its construction, the Hubbard correction applies primarily to the Kohn–Sham orbitals that have the most overlap with the LOs; viewed another way, the (spatially) localized orbitals that have the most energy-local character (via their large overlap with energy eigenstates). [96] In particular, the d and f atomic orbitals of transition metals correspond closely to flat bands in reciprocal space, which carry some energy information implicitly. However, they are independent of the of the system's geometry. In contrast, the LOs of LOSC are dynamic: the orbitals can change with the geometric structure of the system. This is key to their utility in finite systems. In compact structures near equilibrium, the LOSC LOs can replicate the Kohn–Sham canonical orbitals, while becoming localized as chemical bonds are stretched. This allows the LOSC total energy correction to change with the geometry, as seen in Li *et al.* [43] and Su *et al.* [44]

Neither sLOSC nor DFT+U are suitable for solving the analogue of delocalization error for systems with fractional spin. [14, 22] For molecules, fractional-spin LOSC (FSLOSC) [91] extends the original LOSC method to this case; the judiciously modified DFT (jmDFT) method [97, 98] does the same for DFT+U.

2. Koopmans-compliant functionals

Koopmans-compliant functionals [99, 100] mitigate delocalization error by enforcing the PPLB linearity condition directly: in the Koopmans integral (KI) formulation, [39]

$$\Delta E_{\mathrm{KI}} = \sum_i \alpha_i \left[f_i \eta_i - \int_0^{f_i} ds_i \, \langle \phi_i | h_s(s_i) | \phi_i \rangle \right]. \quad (29)$$

Here α_i is an orbital-dependent screening function based on the relaxation of the LOs ϕ_i; f_i is the (fractional) occupation of ϕ_i; $\eta_i = \int_0^1 ds_i \, \langle \phi_i | h_{\mathrm{PZ}}(s_i) | \phi_i \rangle$, integrating the Perdew–Zunger self-interaction corrected Kohn–Sham Hamiltonian, [32] gives the linearized slope of the energy with respect to f_i; and the last term computes the nonlinearity in E that is replaced by $f_i \eta_i$. Like (s)LOSC, Koopmans-compliant functionals are dependent on the choice of localized orbitals. [101] In extended systems, localized orbitals are necessary for a Koopmans-compliant correction to have any effect, [80] and screening has also been found to effect improvements in band gap calculation. [79, 81]

An advantage of sLOSC over the Koopmans-compliant functionals for extended systems is that the DLWFs treat the valence and conduction bands together; on the one hand, DLWFs are empirically robust to increasing the number of conduction bands from which they are constructed, and on the other, sLOSC can in principle be applied to metals without additional modification. For gapped systems, the energy localization inherent in the DLWF cost function enforces separation between the occupied and virtual electronic manifolds without manual input. The system with the smallest gap in our analysis, indium antimonide (InSb, experimental gap 0.23 eV), which is predicted to be gapless by the DFA (and whose sLOSC gap is 0.260 eV) has DLWF occupations $\lambda_{ii}^{\mathbf{RR}} \geq 0.98$ in the valence manifold and ≤ 0.0074 in the conduction manifold. It is conceivable that DLWFs could also serve as effective LOs for Koopmans-compliant methods, even if their subspaces corresponding to the valence and conduction bands are not variational for total Koopmans-compliant energy.

3. Additional methods

The Fermi–Löwdin orbital (FLO) self-interaction correction (SIC), [36, 102, 103] which has its roots in the Perdew–Zunger (PZ) self-interaction correction method, [32] also uses localized orbitals for an energy correction. However, the self-interaction error treated by both FLOSIC and PZ-SIC is well-defined only for one-electron systems; LOSC and its derivatives account for the many-electron nature of delocalization error explicitly. [17]

As mentioned in Su *et al.* [91], the generalized transition state method [41] and the Wannier-function method of Ma and Wang [42] are effective at improving band gap predictions. However, since they do not mix valence and conduction bands to create fractionally occupied orbitals, they cannot change the total energy of the DFA calculation; thus, they cannot restore size-consistency to DFAs and will not be able to capture (for instance) molecular dissociation at the same time as improving band gap predictions. This problem is shared by early Koopmans-compliant methods, which used the Kohn–Sham orbitals as the ϕ_i; it underlies the observation of Nguyen *et al.* [80] that localized orbitals such as Wannier functions are required for Koopmans compliance in extended systems.

B. Computational efficiency

The sLOSC method as implemented in this work scales as $O(N_w^3 N_k)$ for the localization step, $O(N_w^2 N_G)$ for the computation of curvature elements, and $O(N_w N_G \log N_G)$ for the FFT of the DLWF densities. Here, N_G is the number of plane waves in the unfolded supercell, which is N_k times the number of plane waves in the unit cell. Calculating the curvature and energy corrections is the computational bottleneck for the systems evaluated in this work, with wall times for each system reaching a few hours using 16 threads on an Intel Xeon E5-2630v3 processor. The systems that took the longest time were those with the largest number of core states, which have no effect on frontier state corrections; these could be neglected if only a correction to the band gap is desired. The running time was divided fairly evenly between the computation of the matrix elements defined in Eqs. (17, 19a, 19b). We note that the size of the integration domain for these quantities could be reduced from the full Born–von Karman supercell if the relevant DLWF densities are contained in a smaller region. This is supported by the fact that systems that had similar localizations for a 4×4×4 and 6×6×6 **k**-mesh yielded very similar energy corrections.

Along the same lines, we find that for the systems in the test set the correction results are converged with a 6×6×6 **k**-mesh, but this is only necessary to achieve a converged localization. Certain systems exhibit a qualitatively different localization with a smaller 4×4×4 **k**-mesh; however, by decreasing the value of γ in the localization cost function F, a set of DLWFs qualitatively similar to the 6×6×6 case can be obtained.

Some other methods that attempt to address delocalization error in bulk calculations, such as the approach of Ma and Wang [42] and the screened range-separated hybrid functional, [31] rely on supercell self-consistent calculations. These have cubic scaling in the number of electrons, so an unfolded Born–von Karman supercell arising from N_k **k**-points sampling a unit cell with N_w Wannier functions scales as $O(N_k^3 N_w^3)$. Both of the aforementioned methods use Wannier functions as a localized charge representation and rely on manually choosing the Bloch orbitals to comprise the Wannier functions representing the frontier of the occupied space. The sLOSC method uses DLWFs, which naturally supply Wannier functions representing the frontier of the occupied and

unoccupied spaces without the need for manual energy windowing.

[1] W. Kohn, Rev. Mod. Phys. **71**, 1253 (1999), publisher: American Physical Society.

[2] P. Hohenbergand W. Kohn, Phys. Rev. **136**, B864 (1964), publisher: American Physical Society.

[3] W. Kohnand L. J. Sham, Phys. Rev. **140**, A1133 (1965), publisher: American Physical Society.

[4] A. D. Becke, The Journal of Chemical Physics **98**, 5648 (1993).

[5] C. Lee, W. Yang, and R. G. Parr, Phys. Rev. B **37**, 785 (1988), publisher: American Physical Society.

[6] J. P. Perdew, K. Burke, and M. Ernzerhof, Phys. Rev. Lett. **77**, 3865 (1996).

[7] R. Van Noorden, B. Maher, and R. Nuzzo, Nature News **514**, 550 (2014), cg_type: Nature News Section: News Feature.

[8] A. J. Cohen, P. Mori-Sánchez, and W. Yang, Science **321**, 792 (2008), publisher: American Association for the Advancement of Science Section: Special Perspectives.

[9] A. J. Cohen, P. Mori-Sánchez, and W. Yang, Chem. Rev. **112**, 289 (2012), publisher: American Chemical Society.

[10] P. Mori-Sánchez, A. J. Cohen, and W. Yang, Phys. Rev. Lett. **100**, 146401 (2008), publisher: American Physical Society.

[11] T. Koopmans, Physica **1**, 104 (1934).

[12] J. F. Janak, Phys. Rev. B **18**, 7165 (1978), publisher: American Physical Society.

[13] J. P. Perdew, R. G. Parr, M. Levy, and J. L. Balduz, PHYSICAL REVIEW LETTERS **49**, 4 (1982).

[14] A. J. Cohen, P. Mori-Sánchez, and W. Yang, Phys. Rev. B **77**, 115123 (2008).

[15] R. Merkle, A. Savin, and H. Preuss, J. Chem. Phys. **97**, 9216 (1992), publisher: American Institute of Physics.

[16] Y. Zhangand W. Yang, J. Chem. Phys. **109**, 2604 (1998), publisher: American Institute of Physics.

[17] P. Mori-Sánchez, A. J. Cohen, and W. Yang, J. Chem. Phys. **125**, 201102 (2006), publisher: American Institute of Physics.

[18] J. P. Perdew, A. Ruzsinszky, G. I. Csonka, O. A. Vydrov, G. E. Scuseria, V. N. Staroverov, and J. Tao, Phys. Rev. A **76**, 040501 (2007), publisher: American Physical Society.

[19] T. Körzdörfer, S. Kümmel, and M. Mundt, J. Chem. Phys. **129**, 014110 (2008), publisher: American Institute of Physics.

[20] R. O. Jonesand O. Gunnarsson, Rev. Mod. Phys. **61**, 689 (1989), publisher: American Physical Society.

[21] A. D. Becke, J. Chem. Phys. **140**, 18A301 (2014), publisher: American Institute of Physics.

[22] P. Mori-Sánchez, A. J. Cohen, and W. Yang, Phys. Rev. Lett. **102**, 066403 (2009), publisher: American Physical Society.

[23] W. Yang, A. J. Cohen, and P. Mori-Sánchez, J. Chem. Phys. **136**, 204111 (2012), publisher: American Institute of Physics.

[24] A. Savinand H.-J. Flad, International Journal of Quantum Chemistry **56**, 327 (1995), _eprint: https://onlinelibrary.wiley.com/doi/pdf/10.1002/qua.560560417.

[25] A. Savin, in *Theoretical and Computational Chemistry*, Recent Developments and Applications of Modern Density Functional Theory, Vol. 4, edited by J. M. Seminario (Elsevier, 1996) pp. 327–357.

[26] H. Iikura, T. Tsuneda, T. Yanai, and K. Hirao, J. Chem. Phys. **115**, 3540 (2001), publisher: American Institute of Physics.

[27] T. Yanai, D. P. Tew, and N. C. Handy, Chemical Physics Letters **393**, 51 (2004).

[28] O. A. Vydrovand G. E. Scuseria, J. Chem. Phys. **125**, 234109 (2006), publisher: American Institute of Physics.

[29] J.-D. Chaiand M. Head-Gordon, Phys. Chem. Chem. Phys. **10**, 6615 (2008), publisher: The Royal Society of Chemistry.

[30] R. Baer, E. Livshits, and U. Salzner, Annual Review of Physical Chemistry **61**, 85 (2010), _eprint: https://doi.org/10.1146/annurev.physchem.012809.103321.

[31] D. Wing, G. Ohad, J. B. Haber, M. R. Filip, S. E. Gant, J. B. Neaton, and L. Kronik, PNAS **118**, 10.1073/pnas.2104556118 (2021), publisher: National Academy of Sciences Section: Physical Sciences.

[32] J. P. Perdewand A. Zunger, Phys. Rev. B **23**, 5048 (1981), publisher: American Physical Society.

[33] P. Mori-Sánchez, A. J. Cohen, and W. Yang, J. Chem. Phys. **124**, 091102 (2006), publisher: American Institute of Physics.

[34] J. P. Perdew, V. N. Staroverov, J. Tao, and G. E. Scuseria, Phys. Rev. A **78**, 052513 (2008), publisher: American Physical Society.

[35] T. Schmidt, E. Kraisler, L. Kronik, and S. Kümmel, Physical Chemistry Chemical Physics **16**, 14357 (2014), publisher: Royal Society of Chemistry.

[36] M. R. Pederson, A. Ruzsinszky, and J. P. Perdew, J. Chem. Phys. **140**, 121103 (2014), publisher: American Institute of Physics.

[37] T. Schmidtand S. Kümmel, Phys. Rev. B **93**, 165120 (2016), publisher: American Physical Society.

[38] Z.-h. Yang, M. R. Pederson, and J. P. Perdew, Phys. Rev. A **95**, 052505 (2017), publisher: American Physical Society.

[39] G. Borghi, A. Ferretti, N. L. Nguyen, I. Dabo, and N. Marzari, Phys. Rev. B **90**, 075135 (2014).

[40] N. Colonna, N. L. Nguyen, A. Ferretti, and N. Marzari, J. Chem. Theory Comput. **15**, 1905 (2019), publisher:

American Chemical Society.

[41] V. I. Anisimovand A. V. Kozhevnikov, Phys. Rev. B **72**, 075125 (2005), publisher: American Physical Society.

[42] J. Maand L.-W. Wang, Sci Rep **6**, 24924 (2016).

[43] C. Li, X. Zheng, N. Q. Su, and W. Yang, National Science Review **5**, 203 (2018).

[44] N. Q. Su, A. Mahler, and W. Yang, J. Phys. Chem. Lett. **11**, 1528 (2020).

[45] Y. Mei, Z. Chen, and W. Yang, The Journal of Physical Chemistry Letters 10.1021/acs.jpclett.0c03133 (2020), publisher: American Chemical Society.

[46] Y. Mei, N. Yang, and W. Yang, J. Chem. Phys. **154**, 054302 (2021), publisher: American Institute of Physics.

[47] F. Bloch, Z. Physik **52**, 555 (1929).

[48] N. Ashcroftand D. Mermin, *Solid State Physics* (Thomson Press, 2003).

[49] H. J. Monkhorstand J. D. Pack, Phys. Rev. B **13**, 5188 (1976).

[50] G. Wannier, Physical Review **52**, 191 (1937).

[51] J. D. Cloizeaux, Phys. Rev. **129**, 554 (1963), publisher: American Physical Society.

[52] N. Marzariand D. Vanderbilt, Phys. Rev. B **56**, 12847 (1997), publisher: American Physical Society.

[53] J. M. Fosterand S. F. Boys, Rev. Mod. Phys. **32**, 300 (1960), publisher: American Physical Society.

[54] F. Gygi, J.-L. Fattebert, and E. Schwegler, Computer Physics Communications **155**, 1 (2003).

[55] F. Giustinoand A. Pasquarello, Phys. Rev. Lett. **96**, 216403 (2006).

[56] A. Mahler, J. Z. Williams, N. Q. Su, and W. Yang, arXiv:2201.07751 [cond-mat] (2022), arXiv: 2201.07751.

[57] Y. Mei, J. Yu, Z. Chen, N. Q. Su, and W. Yang, J. Chem. Theory Comput. 10.1021/acs.jctc.1c01058 (2022).

[58] X. Zheng, A. J. Cohen, P. Mori-Sánchez, X. Hu, and W. Yang, Phys. Rev. Lett. **107**, 026403 (2011), publisher: American Physical Society.

[59] D. Haitand M. Head-Gordon, J. Phys. Chem. Lett. **9**, 6280 (2018), publisher: American Chemical Society.

[60] Y. Mei, Z. Chen, and W. Yang, arXiv:2106.10358 [physics, physics:quant-ph] (2021), arXiv: 2106.10358.

[61] P. a. M. Dirac, Mathematical Proceedings of the Cambridge Philosophical Society **26**, 376 (1930), publisher: Cambridge University Press.

[62] J. C. Slaterand J. C. Phillips, Physics Today **27**, 49 (1974), publisher: American Institute of Physics.

[63] J. C. Slater, *Quantum Theory of Molecules and Solids*, Vol. IV (McGrow-Hill, 1974).

[64] See Supplemental Material, which includes Refs. [104–113] at [URL will be inserted by publisher] for details about the (s)LOSC correction to the Hamiltonian, disentanglement, implementation of the (screened) Coulomb integral, the sLOSC parameters including the DLWF mixing parameter, and raw sLOSC data.

[65] I. Souza, N. Marzari, and D. Vanderbilt, Phys. Rev. B **65**, 035109 (2001), publisher: American Physical Society.

[66] G. Makovand M. C. Payne, Phys. Rev. B **51**, 4014 (1995).

[67] L. N. Kantorovich, Phys. Rev. B **60**, 15476 (1999), publisher: American Physical Society.

[68] I. Dabo, B. Kozinsky, N. E. Singh-Miller, and N. Marzari, Phys. Rev. B **77**, 115139 (2008), arXiv: 0709.4647.

[69] Y. Liand I. Dabo, Phys. Rev. B **84**, 155127 (2011), publisher: American Physical Society.

[70] G. Onida, L. Reining, R. W. Godby, R. Del Sole, and W. Andreoni, Phys. Rev. Lett. **75**, 818 (1995), publisher: American Physical Society.

[71] M. R. Jarvis, I. D. White, R. W. Godby, and M. C. Payne, Phys. Rev. B **56**, 14972 (1997), publisher: American Physical Society.

[72] C. A. Rozzi, D. Varsano, A. Marini, E. K. U. Gross, and A. Rubio, Phys. Rev. B **73**, 205119 (2006).

[73] L. Hedin, Physical Review series I **139**, 796 (1965), number: 3A Publisher: American Institute of Physics (AIP).

[74] R. Martin, L. Reining, and D. Ceperley, *Interacting Electrons: Theory and Computational Approaches* (Cambridge University Press, 2016).

[75] M. R. Zaghlouland A. N. Ali, ACM Trans. Math. Softw. **38**, 15:1 (2012).

[76] M. R. Zaghloul, ACM Trans. Math. Softw. **42**, 26:1 (2016).

[77] X. Zheng, T. Zhou, and W. Yang, J. Chem. Phys. **138**, 174105 (2013).

[78] D. Zhang, X. Zheng, C. Li, and W. Yang, J. Chem. Phys. **142**, 154113 (2015).

[79] N. Colonna, N. L. Nguyen, A. Ferretti, and N. Marzari, J. Chem. Theory Comput. **14**, 2549 (2018).

[80] N. L. Nguyen, N. Colonna, A. Ferretti, and N. Marzari, Phys. Rev. X **8**, 021051 (2018).

[81] N. Colonna, R. De Gennaro, E. Linscott, and N. Marzari, arXiv (2022), arXiv:2202.08155 [cond-mat, physics:physics].

[82] W. Yang, A. J. Cohen, F. De Proft, and P. Geerlings, J. Chem. Phys. **136**, 144110 (2012).

[83] D. R. Hamann, Phys. Rev. B **88**, 085117 (2013).

[84] M. J. van Setten, M. Giantomassi, E. Bousquet, M. J. Verstraete, D. R. Hamann, X. Gonze, and G. M. Rignanese, Computer Physics Communications **226**, 39 (2018).

[85] P. Giannozzi, S. Baroni, N. Bonini, M. Calandra, R. Car, C. Cavazzoni, D. Ceresoli, G. L. Chiarotti, M. Cococcioni, I. Dabo, A. D. Corso, S. d. Gironcoli, S. Fabris, G. Fratesi, R. Gebauer, U. Gerstmann, C. Gougoussis, A. Kokalj, M. Lazzeri, L. Martin-Samos, N. Marzari, F. Mauri, R. Mazzarello, S. Paolini, A. Pasquarello, L. Paulatto, C. Sbraccia, S. Scandolo, G. Sclauzero, A. P. Seitsonen, A. Smogunov, P. Umari, and R. M. Wentzcovitch, J. Phys.: Condens. Matter **21**, 395502 (2009), publisher: IOP Publishing.

[86] P. Giannozzi, O. Andreussi, T. Brumme, O. Bunau, M. B. Nardelli, M. Calandra, R. Car, C. Cavazzoni, D. Ceresoli, M. Cococcioni, N. Colonna, I. Carnimeo, A. D. Corso, S. d. Gironcoli, P. Delugas, R. A. DiStasio, A. Ferretti, A. Floris, G. Fratesi, G. Fugallo, R. Gebauer, U. Gerstmann, F. Giustino, T. Gorni, J. Jia, M. Kawamura, H.-Y. Ko, A. Kokalj, E. Küçükbenli, M. Lazzeri, M. Marsili, N. Marzari, F. Mauri, N. L. Nguyen, H.-V. Nguyen, A. Otero-de-la Roza, L. Paulatto, S. Poncé, D. Rocca, R. Sabatini, B. Santra, M. Schlipf, A. P. Seitsonen, A. Smogunov, I. Timrov, T. Thonhauser, P. Umari, N. Vast, X. Wu, and S. Baroni, J. Phys.: Condens. Matter **29**, 465901 (2017), publisher: IOP Publishing.

[87] A. A. Mostofi, J. R. Yates, Y.-S. Lee, I. Souza, D. Vanderbilt, and N. Marzari, Computer Physics Communications **178**, 685 (2008).

[88] A. A. Mostofi, J. R. Yates, G. Pizzi, Y.-S. Lee, I. Souza, D. Vanderbilt, and N. Marzari, Computer Physics Communications **185**, 2309 (2014).

[89] G. Pizzi, V. Vitale, R. Arita, S. Blügel, F. Freimuth, G. Géranton, M. Gibertini, D. Gresch, C. Johnson, T. Koretsune, J. Ibañez-Azpiroz, H. Lee, J.-M. Lihm, D. Marchand, A. Marrazzo, Y. Mokrousov, J. I. Mustafa, Y. Nohara, Y. Nomura, L. Paulatto, S. Poncé, T. Ponweiser, J. Qiao, F. Thöle, S. S. Tsirkin, M. Wierzbowska, N. Marzari, D. Vanderbilt, I. Souza, A. A. Mostofi, and J. R. Yates, J. Phys.: Condens. Matter **32**, 165902 (2020).

[90] J. Heyd, J. E. Peralta, G. E. Scuseria, and R. L. Martin, J. Chem. Phys. **123**, 174101 (2005), publisher: American Institute of Physics.

[91] N. Q. Su, C. Li, and W. Yang, PNAS **115**, 9678 (2018).

[92] V. I. Anisimov, J. Zaanen, and O. K. Andersen, Phys. Rev. B **44**, 943 (1991), publisher: American Physical Society.

[93] M. Cococcioniand S. de Gironcoli, Phys. Rev. B **71**, 035105 (2005).

[94] D. D. O'Regan, in *Optimised Projections for the Ab Initio Simulation of Large and Strongly Correlated Systems*, edited by D. D. O'Regan (Springer, Berlin, Heidelberg, 2012) pp. 89–123.

[95] V. L. J. Campoand M. Cococcioni, J. Phys.: Condens. Matter **22**, 055602 (2010).

[96] B. Himmetoglu, A. Floris, S. de Gironcoli, and M. Cococcioni, Int. J. Quantum Chem. **114**, 14 (2014).

[97] A. Bajaj, J. P. Janet, and H. J. Kulik, J. Chem. Phys. **147**, 191101 (2017).

[98] A. Bajaj, F. Liu, and H. J. Kulik, J. Chem. Phys. **150**, 154115 (2019).

[99] I. Dabo, M. Cococcioni, and N. Marzari, arXiv:0901.2637 [cond-mat] (2009), arXiv:0901.2637 [cond-mat].

[100] I. Dabo, A. Ferretti, N. Poilvert, Y. Li, N. Marzari, and M. Cococcioni, Phys. Rev. B **82**, 115121 (2010).

[101] G. Borghi, C.-H. Park, N. L. Nguyen, A. Ferretti, and N. Marzari, Phys. Rev. B **91**, 155112 (2015).

[102] D.-y. Kao, K. Withanage, T. Hahn, J. Batool, J. Kortus, and K. Jackson, J. Chem. Phys. **147**, 164107 (2017), publisher: American Institute of Physics.

[103] K. A. Jackson, J. E. Peralta, R. P. Joshi, K. P. Withanage, K. Trepte, K. Sharkas, and A. I. Johnson, J. Phys.: Conf. Ser. **1290**, 012002 (2019).

[104] Wolfram Research, Inc., Mathematica, Version 12.3.1 (2021).

[105] A. Damle, L. Lin, and L. Ying, J. Chem. Theory Comput. **11**, 1463 (2015).

[106] A. Damle, L. Lin, and L. Ying, Journal of Computational Physics **334**, 1 (2017).

[107] C. Brouder, G. Panati, M. Calandra, C. Mourougane, and N. Marzari, Phys. Rev. Lett. **98**, 046402 (2007), publisher: American Physical Society.

[108] R. W. G. Wyckoff, *Crystal Structures*, 2nd ed. (Wiley, New York, 1973).

[109] F. Tranand P. Blaha, Phys. Rev. Lett. **102**, 226401 (2009), publisher: American Physical Society.

[110] R. T. Poole, J. G. Jenkin, J. Liesegang, and R. C. G. Leckey, Phys. Rev. B **11**, 5179 (1975), publisher: American Physical Society.

[111] D. M. Roesslerand W. C. Walker, Phys. Rev. **166**, 599 (1968), publisher: American Physical Society.

[112] Y. Kanekoand T. Koda, Journal of Crystal Growth **86**, 72 (1988).

[113] Y.-S. Lin, C.-W. Tsai, G.-D. Li, and J.-D. Chai, J. Chem. Phys. **136**, 154109 (2012), publisher: American Institute of Physics.